Research paper

Concentration-dependent effects of CSF1R inhibitors on oligodendrocyte progenitor cells *ex vivo* and *in vivo*

Yiting Liu[a,*], Katherine S. Given[b], Erin L. Dickson[b], Gregory P. Owens[a], Wendy B. Macklin[b,d], Jeffrey L. Bennett[a,c,d,*]

[a] *Department of Neurology, University of Colorado School of Medicine, Aurora, CO, USA*
[b] *Department of Cell & Developmental Biology, University of Colorado School of Medicine, Aurora, CO, USA*
[c] *Department of Ophthalmology, University of Colorado School of Medicine, Aurora, CO, USA*
[d] *Program in Neuroscience, University of Colorado School of Medicine, Aurora, CO, USA*

ARTICLE INFO

ABSTRACT

Microglia are the principal resident immune cells in the central nervous system (CNS) and play important roles in CNS development, maintenance and repair. The survival and development of microglia depends on colony-stimulating factor 1 receptor (CSF1R), a member of the platelet-derived growth factor receptor (PDGFR) family of tyrosine kinases. Recently pharmacological CSF1R inhibition has been used to investigate the effects of microglial depletion in numerous animal models of CNS disease. However, the effects of CSF1R inhibitors on other cell types in the CNS remains incompletely characterized. In this report, we compared the effect of two commonly used CSF1R inhibitors, PLX5622 and PLX3397, on microglia and oligodendrocyte progenitor cell (OPC) numbers. In *ex vivo* cerebellar slices and adult mouse brain, both PLX compounds caused robust microglia loss; the kinetics of microglial depletion was more rapid with PLX5622. While high-doses of PLX5622 and PLX3397 reduced OPC number in primary cultures *in vitro* and *ex vivo*, low-doses of PLX5622 did not affect the number of OPCs or mature oligodendroglia in culture or *in vivo*. In adult mice, treatment with PLX5622 had no effect on OPC numbers for 7 days; however, a mild reduction was observed after 21 days in some CNS regions. In contrast, PLX3397 caused significant OPC loss after 7 days of treatment, despite only modest microglia depletion. Neither PLX compound had a remarkable effect on mature oligodendrocytes or myelin protein expression following long-term oral administration. Our results show that CSF1R inhibition with PLX5622 can selectively deplete microglia *ex vivo* and *in vivo* without affecting OPC number, demonstrating that microglia are not essential for OPC viability in *ex vivo* slice cultures or adult CNS tissues.

1. Introduction

Microglia are the main resident immune-competent cell population of the central nervous system (CNS), and are ubiquitously spread throughout the CNS. They are versatile effectors and regulators for CNS homeostasis during development and aging (Grabert et al., 2016; Matcovitch-Natan et al., 2016) and in pathology (Salter and Stevens, 2017). Survival and development of microglia critically depends on colony-stimulating factor 1 receptor (CSF1R) signaling (Elmore et al., 2014; Spangenberg et al., 2016). CSF1R is a tyrosine kinase belonging

to the platelet-derived growth factor receptor (PDGFR) family of type III receptor tyrosine kinases, which includes PDGFRα and β (Robinson et al., 2000). Recently, several pharmacological CSF1R inhibitors have been developed to effectively deplete microglia, and these reagents have been frequently employed to probe the role of microglia in models of CNS disease (Han et al., 2017).

PLX3397 and PLX5622 (Plexxikon Inc.) are commonly used CSF1R inhibitors. Administration of PLX3397 or PLX5622 in rodent chow depletes approximately 90% of microglia from adult brain and spinal cord in 21 days without functional impairment (Acharya et al., 2016;
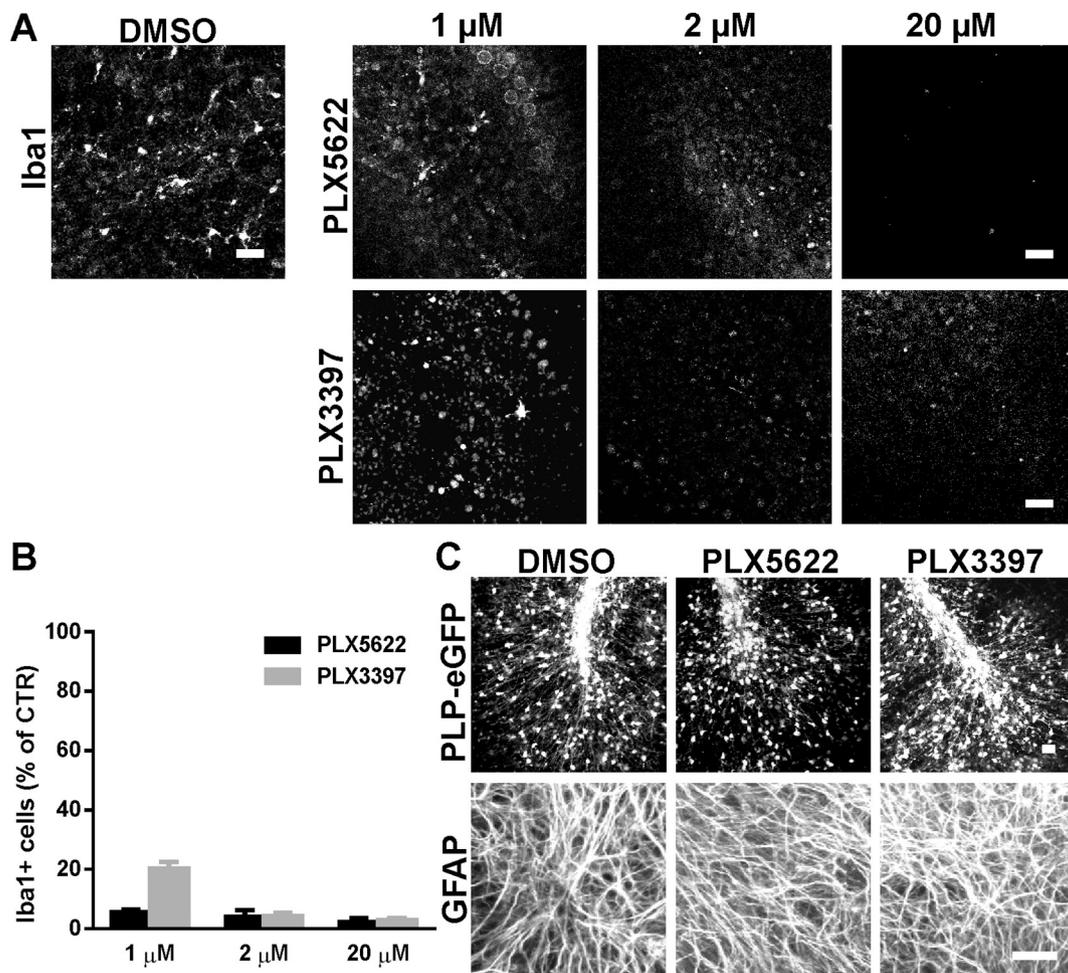
Fig. 1. CSF1R inhibitors PLX5622 and PLX3397 effectively depleted microglia without affecting oligodendrocytes or astrocytes in cerebellar slices. PLX5622 or PLX3397 were applied to cerebellar slices prepared from PLP-eGFP pups at various concentrations as indicated for 3 days. A. Representative confocal images of Iba1 immunostaining in control (DMSO), PLX5622 or PLX3397 treated slices. B. Quantification of the number of Iba1 + cells in slices for all treatment groups. Cell count was normalized to DMSO control (CTR) slice. n = 3–4. C. Confocal images of PLP-eGFP and GFAP immunostaining in slices treated with DMSO or 2 μM PLX5622 or PLX3397. Scale bars: 25 μm.

Elmore et al., 2015; Elmore et al., 2014; Li et al., 2017; Rice et al., 2017; Spangenberg et al., 2016; Szalay et al., 2016). Dose-dependent studies of PLX5622 chow have demonstrated that a low dose (300 mg/kg) resulted in a loss of 30% of the microglia in the cortex following 7 and 21 days of treatment, however, a with a high dose (1200 mg/kg), 80% of microglia are depleted within 7 days and 90% by 21 days of administration (Dagher et al., 2015). Dosing studies with PLX3397 initially used a dose of 1160 mg/kg, which was later titrated to 290 and then 275 mg/kg without any notable differences in microglial depletion (Elmore et al., 2014; Peranzoni et al., 2018). Withdrawal of PLX3397 resulted in rapid microglial repopulation from CNS-resident, nestin-expressing cells (Elmore et al., 2015).

CSF1R inhibitors have variable specificity and can also bind to other type III receptor tyrosine kinases. PLX3397 binds and inhibits CSF1R and c-Kit with a half maximal inhibitory concentration (IC_{50}) of 20 and 10, respectively, as well as inhibiting other kinases *in vitro* (FLT3 and KDR) (DeNardo et al., 2011). PLX5622 is more specific for CSF1R than PLX3397, with at least 50-fold selectivity over 4 related kinases and over 100-fold selectivity against a panel of 230 kinases (Dagher et al., 2015; Kim et al., 2014). Among these kinases, PDGFRα is highly expressed by oligodendrocyte progenitor cells (OPCs) and is essential for their survival (Nishiyama et al., 2009; Tap et al., 2015). Other than *in vitro* assays reporting IC_{50} concentrations against individual kinase molecules, there are few studies that characterize the effects of CSF1R inhibitors on other CNS-resident cells. Indeed, potential off-target

effects of CSF1R inhibitors on other receptor tyrosine kinases may explain the variabilities observed following microglial depletion in different animal models (Han et al., 2017).

In this study, we compared the effects of two common CSF1R inhibitors, PLX3397 and PLX5622, on microglia elimination and OPC cell number in *ex vivo* cerebellar slice cultures and *in vivo* adult brain. We observe that both PLX compounds can significantly reduce the numbers of OPCs in a dose dependent manner in cerebellar slices. However, *in vivo*, we revealed significant differences between PLX5622 and PLX3397 in the efficacy of microglia depletion and effects on OPCs. Our results demonstrate that complete and selective depletion of microglia may be achieved using low doses of PLX5622 *ex vivo* or short term administration *in vivo*. In addition, our results demonstrate that microglia are not essential for OPC viability in *ex vivo* slice cultures or adult CNS tissues.

2. Materials and methods

2.1. Animals

The care and euthanasia of animals are in accordance with University of Colorado IACUC policy for animal use and the NIH Guide for the Care and Use of Laboratory Animals.
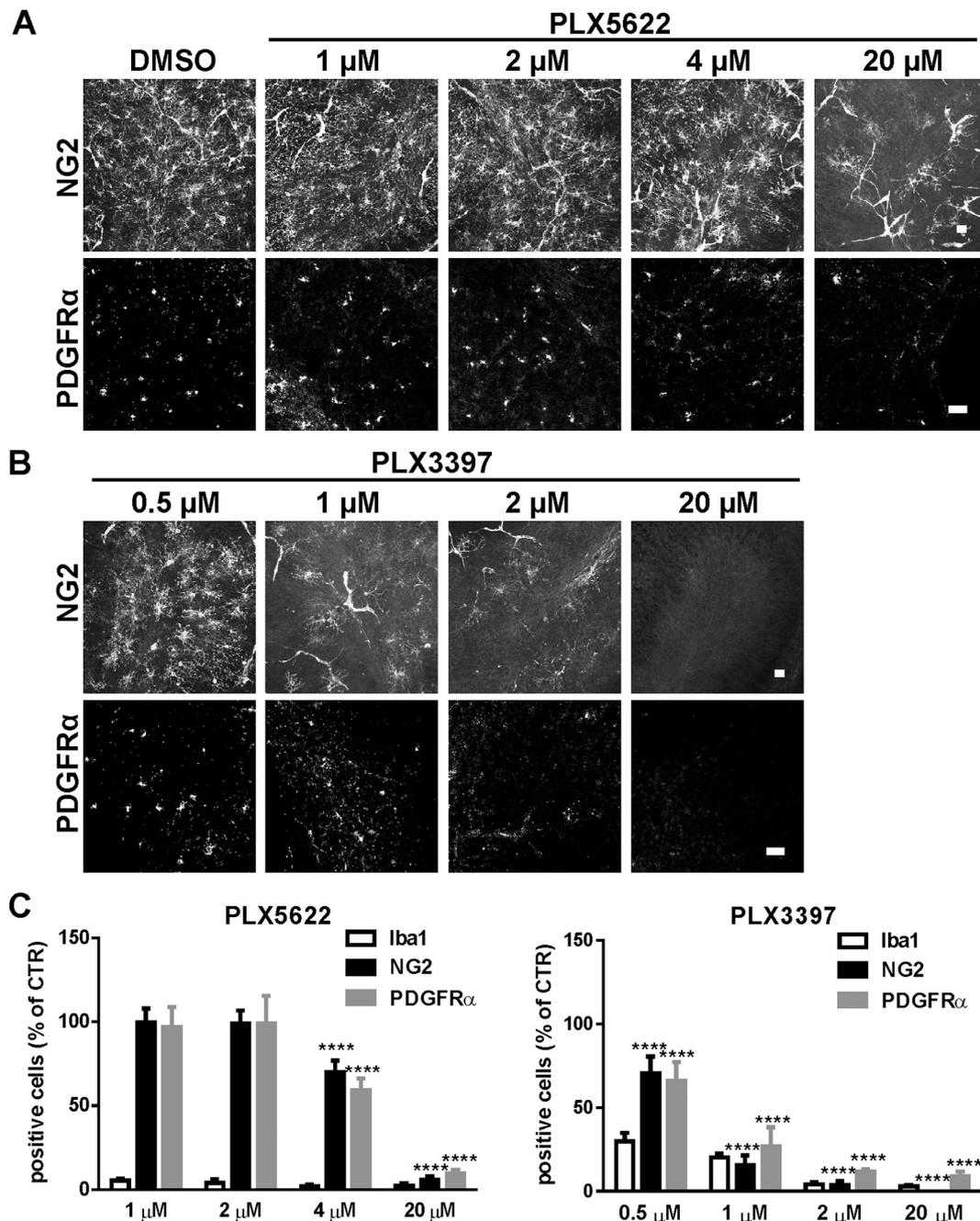
Fig. 2. PLX5622 and PLX3397 demonstrated dose-specific effects on OPC cell number. A, B. Representative confocal images of NG2 or PDGFRα immunostaining in slices treated with control (DMSO), PLX5622 and PLX3397 at the indicated concentrations for 3 days. C, D. Quantification of the number of NG2 + or PDGFRα + cells for all groups in slices. Cell count was normalized to the DMSO control (CTR) slice. Statistical analyses were performed by unpaired Student's *t*-test. ****: *p* < .0001, n = 3–4. Scale bars: 25 μm.

2.2. Compounds

PLX5622 and PLX3397 stock solutions were provided by Plexxikon Inc. at 20 mM in dimethyl sulfoxide (DMSO). Mouse chows were formulated in AIN-76A standard chow by Research Diets Inc. at 1200 mg/kg for PLX5622 and 275 mg/kg for PLX3397.

2.3. Cerebellar slice culture

Sagittal cerebellar slices (300 μm) were prepared from PLP-eGFP mice (Mallon et al., 2002) at P10–12 and cultured on MilliCell 0.4 μm membrane inserts (Millipore, Billerica, MA) in slice media: 25% Hank's balanced salt solution (HBSS), 25% heat-inactivated horse serum, 50%

minimum essential media (MEM), 125 mM HEPES, 28 mM D-Glucose, 2 mM L-Glutamine, 10 U/ml penicillin/streptomycin, all from Life Technologies, Carlsbad, CA) at 37 °C (Sheridan and Dev, 2012). Media was changed within the first 24 h of plating, and then every 2–3 days. Slices were cultured for 7–10 days prior to treatment. DMSO, PLX5622 and PLX3397 were applied at indicated concentrations in slice media for 3 or 8 days. Media was changed every 2–3 days. Following treatment, slices were rinsed once in PBS, fixed in 4% PFA in PBS for 30 min, and subjected to immunostaining.

2.4. Animal chow treatment

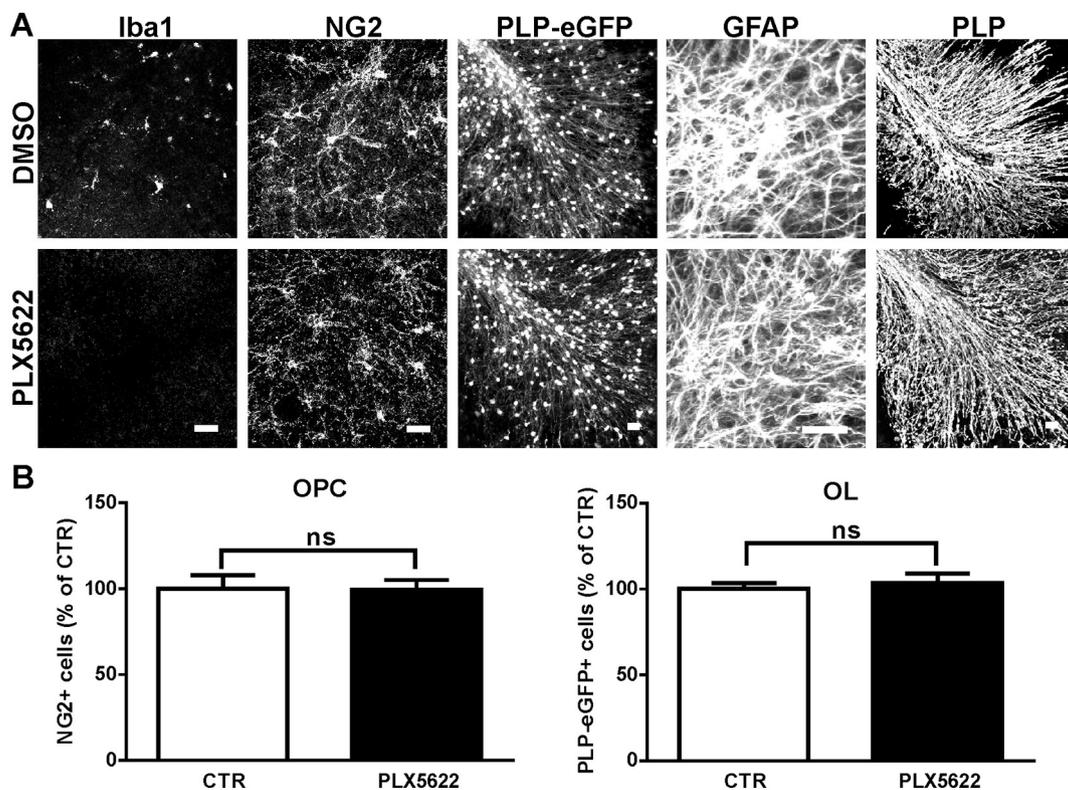Male and female PLP-eGFP animals (4–5 per group) aged

Fig. 3. Selective microglia depletion in slices after extended PLX5622 treatment had no effect on mature oligodendrocytes, astrocytes, or myelin protein. A. Slices were treated with control (DMSO) or 2 μM PLX5622 for 8 days, stained and imaged for Iba1, NG2, PLP-eGFP, GFAP and myelin protein PLP. B. Quantification of the number of NG2 + and PLP-eGFP + cells in slices. Cell count was normalized to the DMSO control (CTR) slice. Statistical analyses were performed by unpaired Student's *t*-test. ns: no significance, $n = 3$. Scale bars: 25 μm.

8–12 weeks were placed on formulated PLX Chow (1200 mg/kg for PLX5622 and 275 mg/kg for PLX3397) or standard diet for 7 or 21 days. Following treatment, animals were perfused with ice cold PBS followed by 4% paraformaldehyde in PBS. Brains and spinal cords were dissected, post-fixed overnight and then cryoprotected. Tissues were sectioned at 30um on a cryostat and collected in PBS for free-floating immunostaining.

2.5. Immunostaining

For immunohistochemistry, explants or free-floating tissue sections were rinsed in PBS. For myelin proteins, tissues were permeabilized 10% Triton X-100 in PBS (PBSTx) for 20 min and then rinsed in PBS. Tissues are blocked with 5% normal donkey serum (NDS) in PBSTx (1%) for 1 h, and then incubated with primary antibodies overnight at room temperature. Following 3, 10 min washes in PBS, Alexa Fluor-labeled secondary antibodies (Jackson ImmunoResearch, West Grove, PA) were applied (1:800) 2 h at room temperature, washed 3 times for 10 min in PBS, mounted on slides with water, dried and cover-slipped with Fluoromount G (Southern Biotech, Birmingham, AL). The following primary antibodies were used: Rat anti-PLP 1:100 (Yamamura et al., 1991), Rabbit anti-S100b 1:500 (Sigma, S2644), Rabbit anti-GFAP 1:1000 (Sigma, G9269), Goat anti-Iba1 1:400 (Abcam, ab5076), Guinea Pig anti-NG2 1:2000, Rabbit anti-NG2 1:2000, and Rabbit anti-PDGFRa 1:500 (Gifts from William Stallcup, Burnham Institute).

2.6. Microscopy

Images were acquired with either a Leica SP5 laser scanning confocal microscope (Leica Microsystems GmbH, Wetzlar, Germany) or Zeiss Axio-Imager epi-fluorescence microscope (Carl Zeiss Microscopy, Thornwood, NY). At least 4 sections from similar regions of each

explant section, brain or spinal cord were imaged with identical settings.

2.7. Purified primary OPC cell culture

Primary murine OPC culture was prepared from PLP-eGFP pups as described (Liu et al., 2016). Briefly, mixed glial cultures were prepared from P0-1 dissociated cortices and plated on poly-D-lysine (Sigma) coated T75 flask. Purified OPC monocultures were prepared by shaking flasks of confluent mixed glial cultures overnight at 200 rpm to detach the OPCs. OPCs were plated on poly-D-lysine/laminin (Sigma) coated dishes and maintained in media containing 10 ng/ml PDGF (platelet-derived growth factor)/FGF (fibroblast growth factor) (Peprotech, Rocky Hill, NJ) for 24–48 h prior to experiments.

2.8. IncuCyte live cell imaging

Live cell imaging was performed using IncuCyte Zoom from Essen BioScience (Ann Arbor, MI) as described (Liu et al., 2016). Cells were grown and scanned on 24-well plates in the cell culture incubator. Each well was scanned with a 10× objective lens in 9 randomly selected positions at 15 min intervals with high definition phase contrast and epifluorescence microscopy using the 585/635 nm filter (red fluorescence, to detect the DRAQ7 dead cell nuclei; Cell Signaling Technology, Danvers, MA). Image processing and cell counting were performed using IncuCyte and ImageJ software.

2.9. Quantification and statistical analysis

Confocal and fluorescence microscope images were quantified manually with ImageJ (National Institutes of Health open source). For *ex vivo* cerebellar slices, 2–3 images of folia were taken, quantified, and
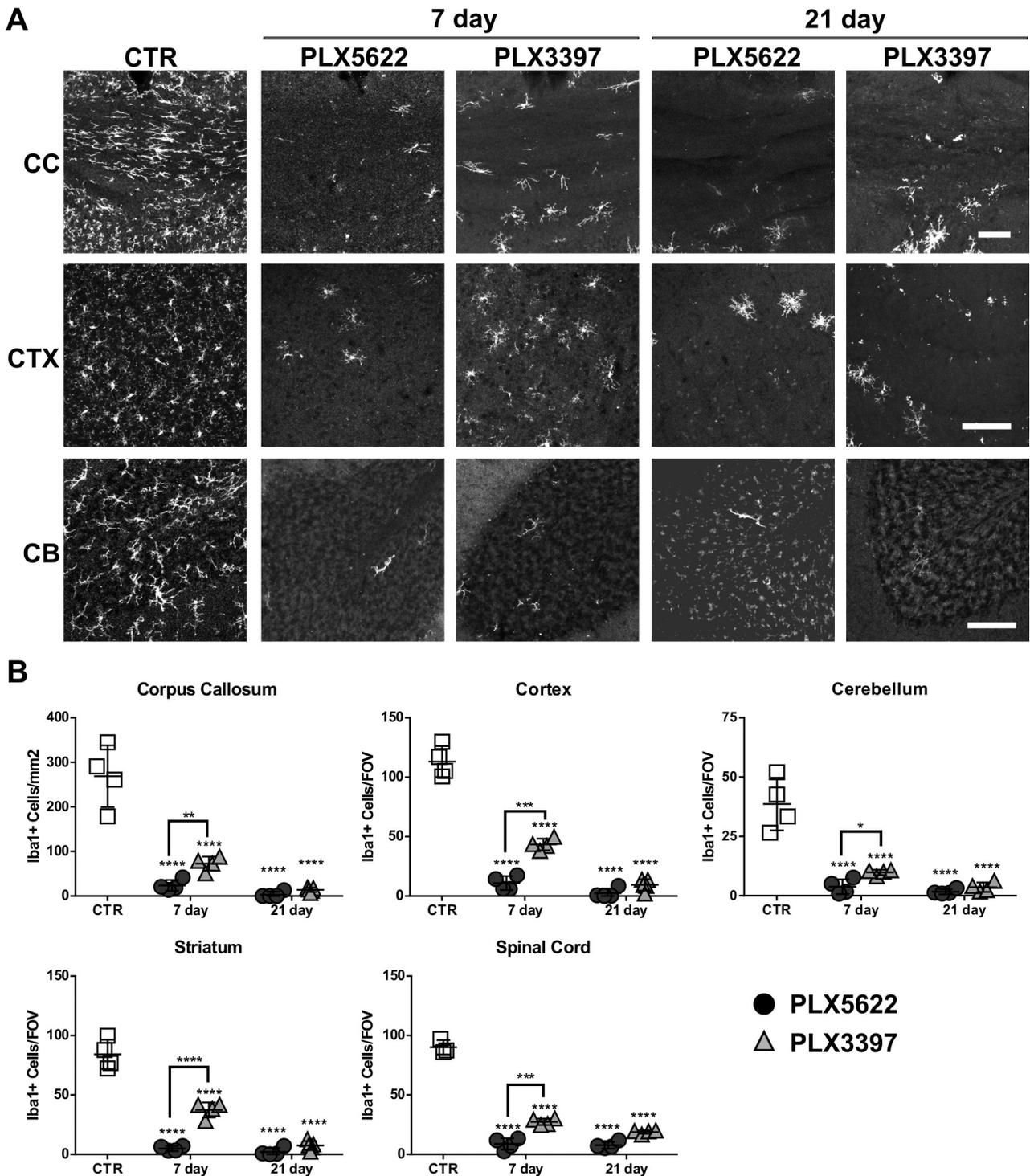
Figure 4

Fig. 4. PLX5622 or PLX3397 chow eliminated microglia in the CNS of adult mice. Adult PLP-eGFP mice aged 8–10 weeks old were fed either control chow or chow containing 1200 mg/Kg PLX5622 or 275 mg/Kg PLX3397 for 7 or 21 days. A. Representative confocal images of Iba1 immunostaining in corpus callosum (CC), cortex (CTX) and cerebellum (CB) of control mice (CTR), PLX5622-treated, or PLX3397-treated animals. B. Quantification of the number of Iba1 + cells for all groups in corpus callosum (CC), cortex (CTR), cerebellum (CB), striatum (STR) and spinal cord (SC). For corpus callosum, the number of positive cells was presented per mm^2 in the region of interest (ROI). For other regions, the number of positive cells in each field of view (FOV) is reported. Statistical analyses were performed by one-way ANOVA between PLX treated groups at 7 days or 21 days and control (CTR), and by unpaired Student's t-test for comparisons between PLX5622 and PLX3397 at 7 days. *: $p < .05$, **: $p < .01$, ***: $p < .001$, ****: $p < .0001$, $n = 4$. Scale bars: 100 μm.

averaged. Slices from 3 to 4 independent experiments were analyzed. For *in vivo* chow experiments, at least 4 sections of brains and spinal cords were imaged in each region (cortex above hippocampus, midline corpus callosum, striatum, and cerebellum), quantified manually using ImageJ cell counter, and averaged. To quantify PLP fluorescence, the mean fluorescence intensity (MFI), area and integrated density of the

Table 1
Effect of PLX chow on microglia depletion and OPC reduction in various CNS regions in adult mice.

		PLX 5622		PLX 3397	
		Microglia depleted	OPC reduction	Microglia depleted	OPC reduction
7d	CC	91.2 ± 4.6%	None	72.9 ± 5.8%	None
	CTX	90.3 ± 5.2%	None	61.6 ± 4.3%	32.1 ± 1.5%**
	STR	94.2 ± 2.4%	None	55.6 ± 7.5%	35.9 ± 0.9%**
	CB	90.2 ± 8.1%	None	74.5 ± 2.9%	None
	SC	90.3 ± 5.4%	None	69.6 ± 3.0%	33.2 ± 6.9%****
21d	CC	98.8 ± 2.5%	None	94.8 ± 1.8%	None
	CTX	97.9 ± 3.6%	30.4 ± 11.0%**	91.7 ± 4.2%	41.8 ± 5.4%****
	STR	97.5 ± 3.9%	28.8 ± 5.2%**	91.2 ± 4.5%	42.7 ± 7.4%****
	CB	95.7 ± 2.7%	22.5 ± 11.6%*	90.7 ± 5.2%	24.5 ± 13.3%*
	SC	91.5 ± 3.1%	22.8 ± 4.3%**	79.1 ± 1.7%	36.4 ± 2.1%****

Percentage was calculated to control animals. Statistical analyses were performed by one-way ANOVA between PLX treated groups at 7 days or 21 days and control. *: $p < .05$, **: $p < .01$, ****: $p < .0001$, n = 4.

signal were measured from a region of interest (ROI) in the corpus callosum and cortex, and from an area with no fluorescence (background) using ImageJ. The MFI of the signal was subtracted by the MFI of the background. The corrected total fluorescence (CTF) was calculated as follows: CTF = Integrated density – (MFI of the background x Area of the signal) (Leite et al., 2014). Statistical analyses were performed by unpaired Student's t-test for single comparisons, one-way ANOVA, or two-way ANOVA for grouped comparisons using GraphPad Prism software. Data are expressed as means ± SD of independent experiments ($n \geq 3$). Significance is reported for $p < .05$.

3. Results

3.1. CSF1R kinase inhibitors PLX5622 and PLX3397 depleted microglia in cerebellar slices

PLX5622 or PLX3397 were applied to cerebellar slices at increasing concentrations from 1 to 20 μM. After three days of treatment, both PLX5622 and PLX3397 at concentrations > 2 μM eliminated > 95% of microglia (Fig. 1A,B). At 1 μM, PLX5622 caused 15% more depletion than PLX 3397 (94.6 ± 1.1% vs 79.9 ± 2.4% Iba1+ cell loss) (Fig. 1A,B). With > 95% loss of microglia at 2 μM, no changes were observed in the viability or morphology of oligodendrocytes or astrocytes, as assessed by PLP-eGFP expression or GFAP staining with either PLX preparation (Fig. 1C).

3.2. High concentrations of PLX5622 and PLX3397 were cytotoxic to OPCs ex vivo and in vitro

Because CSF1R inhibitors may bind to multiple tyrosine kinases, we examined the effects of PLX5622 and PLX3397 on OPCs, which depend on the tyrosine kinase PDGFRα for survival. OPC cell numbers were assessed by NG2 or PDGFRα immunostaining following exposure of cerebellar explants to increasing PLX concentrations for 3 days. At 4 μM, PLX5622 caused a 30–40% reduction in NG2+ or PDGFRα+ cells; this increased to 90–95% at 20 μM. No reduction of NG2+ or PDGFRα+ OPCs was observed in slices exposed to 1 μM or 2 μM PLX5622 despite robust (~95%) depletion of the microglial cells (Fig. 2A,C). In contrast, treatment with PLX3397 significantly reduced OPC numbers at all concentrations tested. We observed a 30–35% loss of NG2+ or PDGFRα+ cells at 0.5 μM, despite incomplete (~70%) depletion of microglia. OPC loss with PLX3397 was concentration dependent with a 75–85% reduction at 1 μM and > 90% loss at 2 μM and 20 μM (Fig. 2B,D).

A similar effect on OPCs was observed in purified primary murine OPC cultures. Cell type specific marker staining showed that the cultures consisted of > 92% OPCs (PDGFRα), < 1% astrocytes (GFAP), and 3.7 ± 2.1% microglia (Iba1) (Supplemental Fig. S1A). Most

oligodendroglial cells were OPCs but, occasionally (< 0.5%) maturing OLs (O4+ with a highly complex network of processes) were noted (data not shown). Low concentration (0.5 μM) of PLX5622 had no effect on viability after 24 h; however, 20 μM PLX5622 resulted in increased OPC death. In contrast, PLX3397 treatment caused significant cytotoxicity at 0.5 μM and 20 μM (Supplemental Fig. S1B,C). These results indicate that the PLX CSF1R inhibitors can directly impair OPC viability in a concentration-dependent manner.

To examine the effect of long-term microglia depletion on OPC survival, 2 μM PLX5622 was applied to cerebellar slices for 8 days. Although microglia were completely eliminated, we observed no difference in NG2+ cell numbers when compared to DMSO-treated controls. In addition, long-term exposure to PLX5622 had no effect on the morphology or number of oligodendrocytes (assessed by PLP-eGFP) and astrocytes (assessed by GFAP and S100b) (Fig. 3A,B and data not shown). Myelin protein expression (measured by PLP immunofluorescence) was unchanged (Fig. 3A).

In concert, both ex vivo and in vitro data demonstrate that low concentrations (≤ 2 μM) of PLX5622 completely deplete microglia in the absence of direct effects on OPCs, oligodendrocytes or astrocytes. PLX3397 causes a significant reduction in viable OPCs even at low concentrations. At higher concentrations, both PLX compounds diminish OPC cell numbers in primary cell culture and cerebellar slices.

3.3. PLX5622 and PLX3397 effectively depleted microglia in adult mouse CNS

We next examined the extent of microglia depletion in various brain regions of adult mice using pre-manufactured chow containing PLX5622 (1200 mg/kg) or PLX3397 (275 mg/kg) for 7 or 21 days. These doses were the lowest ones of each drug to give maximal microglia depletion based on previous studies in the literature (Elmore et al., 2015; Elmore et al., 2014; Peranzoni et al., 2018; Rice et al., 2017; Spangenberg et al., 2016; Szalay et al., 2016). Consistent with prior studies, we observed a rapid decrease in the number of Iba1+ microglia in the corpus callosum (CC, 91.2 ± 4.6%), cortex (CTX, 90.3 ± 5.2%), cerebellum (CB, 90.2 ± 8.1%), striatum (STR, 94.2 ± 2.4%) and spinal cord (SC, 90.3 ± 5.4%) following 7 days of treatment with PLX5622 (Fig. 4 and Table 1). After 21 days, > 95% of microglia were eliminated from most brain regions and 91.5 ± 3.1% were depleted from spinal cord (Fig. 4 and Table 1). Microglia depletion with PLX3397 demonstrated a slower time course than PLX5622. After 7 days of PLX3397 chow, we observed ~70% loss of Iba1+ cells in corpus callosum, cerebellum and spinal cord, and ~55–60% in cortex and striatum. After 21 days of PLX3397 chow, ~90% of Iba1+ cells were depleted in the brain and ~80% were depleted in the spinal cord (Fig. 4 and Table 1). Thus, both PLX compounds effectively deplete
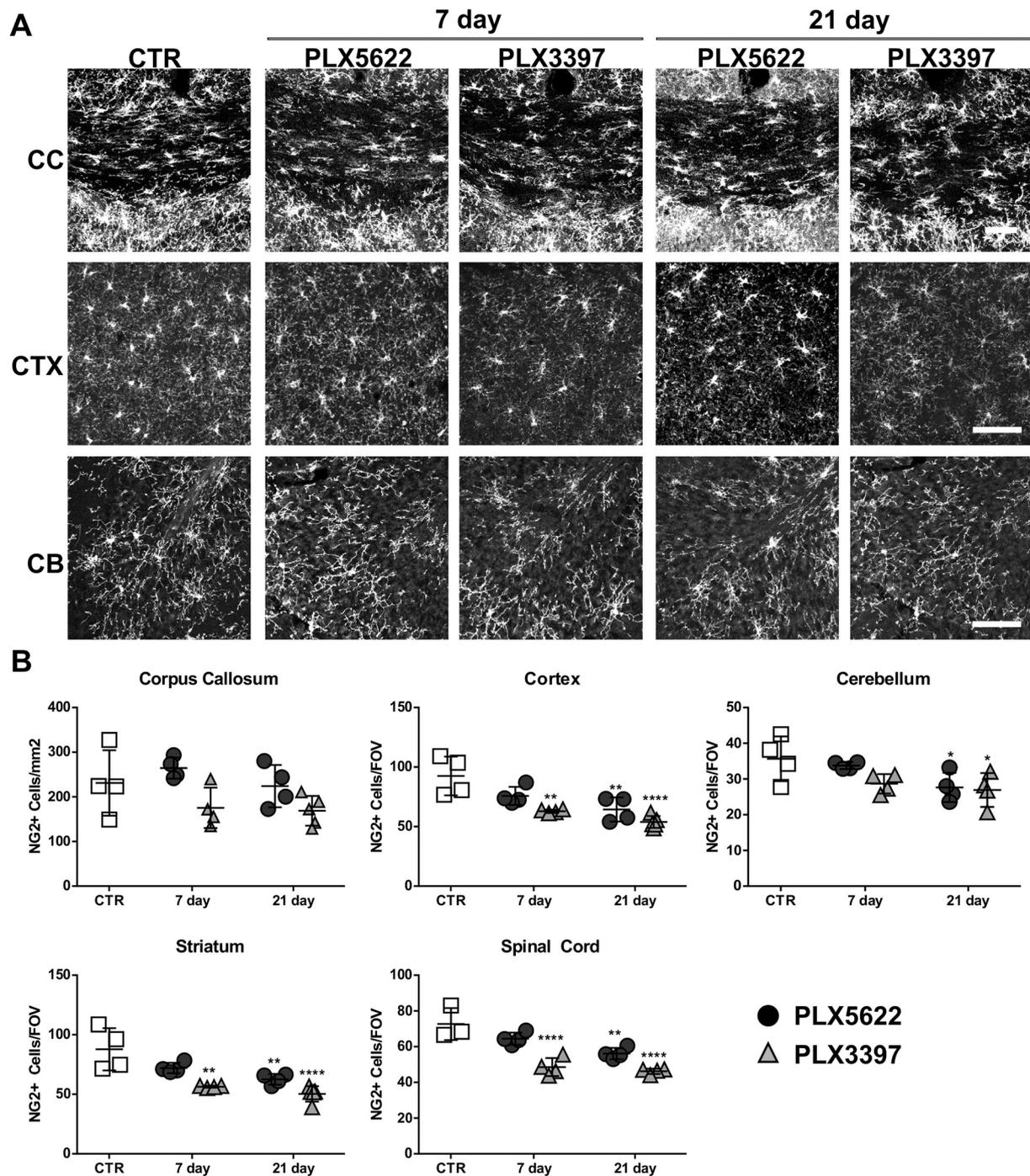
Fig. 5. PLX5622 and PLX3397 chow showed variable effects on OPC number in adult mouse CNS. Adult PLP-eGFP mice aged 8–10 weeks old fed either control chow or chow containing 1200 mg/Kg PLX5622 or 275 mg/Kg PLX3397 for 7 or 21 days. A. Representative confocal images of NG2 immunostaining in corpus callosum (CC), cortex (CTX) and cerebellum (CB) of control mice (CTR), PLX5622-treated, or PLX3397-treated animals. B. Quantification of the number of NG2+ cells for all groups in corpus callosum (CC), cortex (CTR), cerebellum (CB), striatum (STR) and spinal cord (SC). For corpus callosum, the number of positive cells was presented per mm^2 in the region of interest (ROI). For other regions, the number of positive cells in each field of view (FOV) is reported. Statistical analyses were performed by one-way ANOVA between PLX treated groups at 7 days or 21 days and control (CTR). *: $p < .05$, **: $p < .01$, ****: $p < .0001$, $n = 4$. Scale bars: 100 µm.

microglia *in vivo*, although the effect of PLX5622 is more rapid than PLX3397 using the study dosages.

3.4. PLX compounds showed differential effects on OPC viability in vivo

We evaluated the effect of PLX treatment on OPCs *in vivo* by quantifying NG2+ cells in brain and spinal cord. Following 7 days of PLX5622 treatment, we observed no significant reduction in NG2+ cell numbers in any CNS region despite a near complete loss of microglia. However, following extended treatment for 21 days, a mild decline in NG2+ cells was detected in cortex (CTX, 30.4 ± 11.0%), striatum (STR, 28.8 ± 5.2%), cerebellum (CB, 22.5 ± 11.6%) and spinal cord (SC, 22.8 ± 4.3%); no change was noted in the corpus callosum (Fig. 5 and Table 1). Treatment with PLX3397 caused a more rapid and significant reduction in OPC cell numbers. After 7 days of treatment, NG2+ cells were decreased in cortex (CTX, 32.1 ± 1.5%), striatum
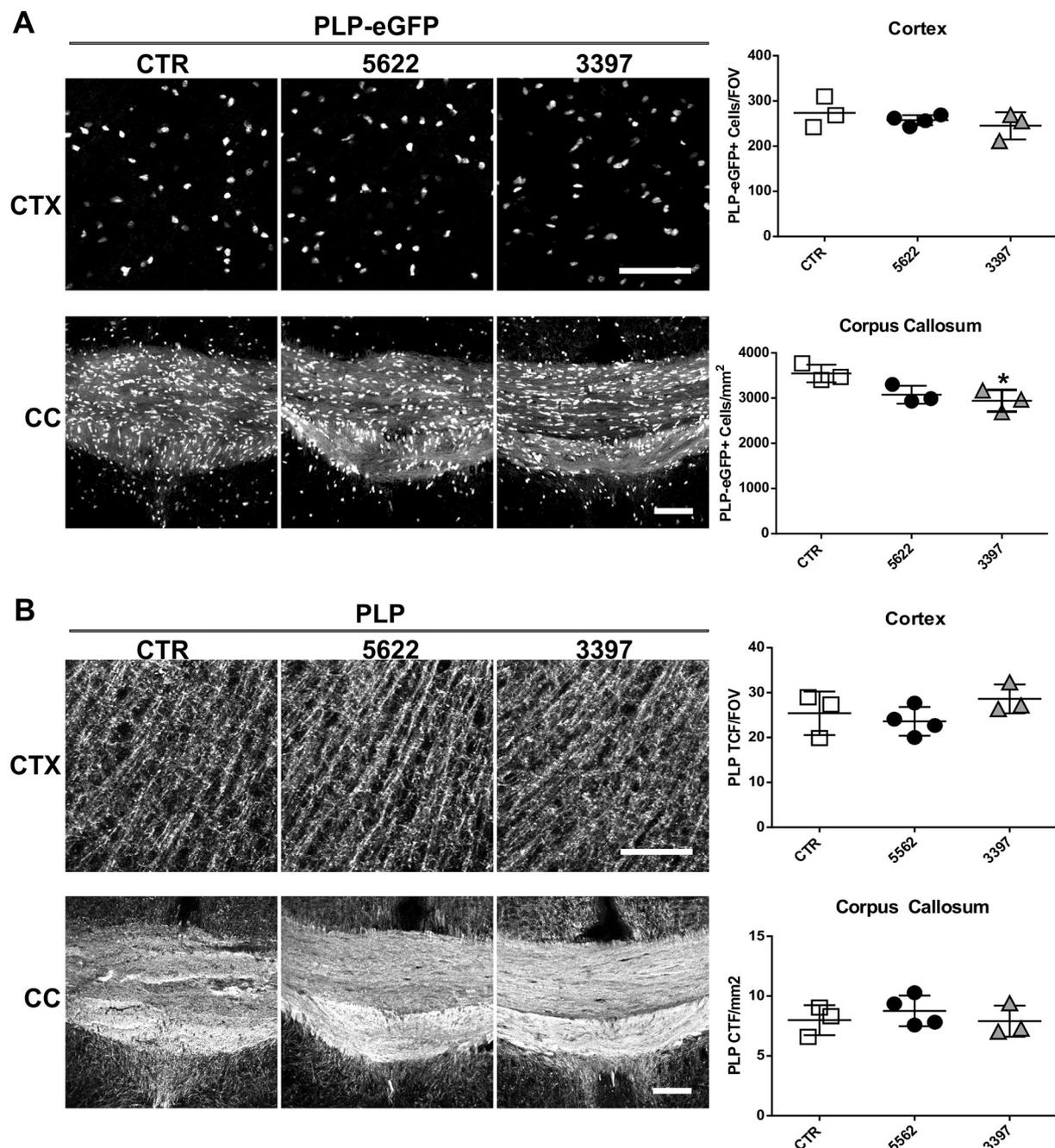
Fig. 6. PLX5622 or PLX3397 chow had no effect on oligodendrocyte cell number or myelin protein at 21 days. Representative confocal images and quantifications of (A) PLP-eGFP and (B) PLP corrected total fluorescence (CTF) in cortex (CTX, upper panels) and corpus callosum (CC, lower panels) of animals fed either control chow or chow containing 1200 mg/Kg PLX5622 or 275 mg/Kg PLX3397 for 21 days. Statistical analyses were performed by one-way ANOVA between PLX treated groups and control (CTR). *: $p < .05$, n = 4. Scale bars: 100 μm.

(STR, 35.9 ± 0.9%) and spinal cord (SC, 33.2 ± 6.9%) (Fig. 5 and Table 1). NG2+ cell loss continued in these regions when treatment was extended to 21 days (Fig. 5 and Table 1). Similar to treatment with PLX5622, NG2+ cell counts were not changed in the corpus callosum following PLX3397 administration. Similar results were obtained when OPCs were quantified using PDGFRα+ staining. Most NG2+ cells were PDGFRα+ (Supplemental Fig. S2A), and PDGFRα+ OPCs were reduced by PLX treatment (Supplemental Fig. S2B). It should be noted that the levels of PLX3397 reached in mice in this study with chow (typical AUC0–24 [area under the plasma concentration-time curve during 24 h] exceeding 1,000,000 ng·h/mL) are much higher than that in patients (AUC0–24–100,000 ng·h/mL) (Plexxikon Inc.).

3.5. Microglia depletion did not affect oligodendrocyte number or myelin expression

We also examined oligodendrocyte cell numbers and myelin proteins following 21 days of PLX treatment. Although > 90% of microglia were ablated in the majority of CNS regions (Table 1), there was no significant change in mature oligodendrocyte cell numbers (PLP-eGFP +) following treatment with PLX5622; a mild reduction (~17%) was observed in the corpus callosum of animals treated with PLX3397 chow (Fig. 6A). Similarly, no difference was observed in myelin protein expression in the cortex and corpus callosum as analyzed by PLP fluorescence intensity (Fig. 6B). Thus, CSF1R inhibition by PLX5622 or PLX3397 did not significantly reduce mature oligodendrocyte cell

number or myelin homeostasis in adult mice.

4. Discussion

In this study, we compared the ability of the CSF1R inhibitors PLX5622 and PLX3397 to ablate microglia in *ex vivo* cerebellar slice cultures and *in vivo* adult mouse CNS. Although both compounds effectively eliminated > 90% of Iba1 + microglia, depletion by PLX5622 was quicker and more robust. Furthermore, PLX5622 had no detrimental effect on OPC numbers *ex vivo* and after 7 days *in vivo*. In contrast, PLX3397 directly impaired OPC viability *in vitro* and caused a reduction in OPC numbers *ex vivo* and *in vivo*.

Both PLX5622 and PLX3397 are potent inhibitors of CSF1R tyrosine kinase with *in vitro* IC_{50} of 10 nM and 20 nM, respectively (Plexxikon Inc.) (DeNardo et al., 2011; Kim et al., 2014). Consistent with these values, significantly lower concentrations of PLX5622 were required for microglial depletion in *ex vivo* cerebellar slice cultures (Fig. 1). *In vivo*, chow containing PLX5622 (1200 mg/Kg chow) depleted > 90% CNS microglia in 7 days, while chow containing PLX3397 (275 mg/Kg chow) required 21 days to reach equivalent depletion (Fig. 4 and Table 1). The rapidity of *in vivo* microglial depletion using PLX5622-chow likely reflects the combination of enhanced potency, dosing and differential pharmacokinetics/CNS penetration. The rapidity and efficacy of microglial depletion *in vivo* depends not only on the binding affinity for the CSF1R receptor, but also on gut absorption, metabolism, excretion, and CNS penetration/retention of the compound. Indeed, a recent report found that four times the dosage of PLX5622 in chow was needed to double the drug concentration in plasma and brain tissue (Nissen et al., 2018).

Reports have noted that PLX5622 is more selective for CSF1R than PLX3397. PLX5622 binds with 50-fold to 100-fold higher affinity to CSF1R than to related kinases (Dagher et al., 2015; Kim et al., 2014; Tap et al., 2015). CSF1R is a member of the PDGFR family of type III receptor tyrosine kinases which includes PDGFRα and ß (Robinson et al., 2000), and PDGFRα signaling is critical for OPC development and maintenance (Nishiyama et al., 2009). The low binding affinity of PLX5622 for PDGFRα likely explains why this compound does not affect OPC viability l at low concentration *in vitro, ex vivo* or *in vivo* (7 days). At high concentrations *in vitro* and *ex vivo*, or following extended administration *in vivo*, both PLX compounds reduce OPC numbers independent of the extent of microglial depletion.

The *in vivo* results are additionally complicated by drug pharmacokinetics. Extended therapy likely leads to accumulation of drug in the CNS, facilitating off-target binding and inhibition of PDGFRα on OPCs. Indeed, the low IC_{50} of PLX3397 for PDGFR results in dissociation of the relationship between depletion of microglia and OPCs *in vivo* (Fig. 5 and Table 1). Alternative dosing strategies might allow for prolonged *in vivo* microglial depletion without effects on OPCs. Our results demonstrate the need for caution in interpreting the functions of microglia using CSF1R inhibitors. Variable, and even contradictory findings, using CSF1R inhibitors are likely due to differences in dosing, target affinity, and pharmacokinetics that drive off-target effects on CNS cell populations. (reviewed in (Han et al., 2017)).

PLX5622 rapidly eliminates microglia in *ex vivo* cerebellar slice cultures at low concentrations (1 and 2 μM) without affecting OPCs (Fig. 3). *In vivo*, microglia are reduced by > 90% but OPC numbers are unaffected in animals fed PLX5622 chow for 7 days. In contrast, mice fed PLX3397 chow for 7 days showed a significant loss in OPC numbers despite only a partial depletion in microglia (Figs. 4-5). In *ex vivo* cerebellar slice cultures, 2 μM PLX5622 resulted in > 95% depletion of microglia by 3 days yet showed no impact on OPC numbers at 8 days (Figs. 1 and 2). The lack of correlation between microglia depletion and OPC loss following *ex vivo* or *in vivo* administration of PLX compounds further supports the contention that the diminished number of viable OPC is not a direct effect of microglia depletion. Moreover, the lack of a long-term impact on oligodendrocyte cell number or myelin protein

level in PLX5622-treated mice argues against microglia playing a vital role in oligodendrocyte homeostasis in the adult mouse CNS.

Following oral administration of the CSF1R inhibitor BLZ945 to newborn pups for 7 days, Hagenmeyer and colleagues reported coincident microglial depletion and reduced OPC numbers in corpus callosum, cortex and cerebellum. However, in BLZ945-treated adult mice, diminished OPC numbers were detected only in the corpus callosum, despite significant microglial depletion in the cerebellum. The effect of BLZ treatment on OPC numbers was not reported in other CNS regions (Hagemeyer et al., 2017). Similar to our results, neither oligodendrocyte cell number nor myelin protein levels were diminished. While these results may indicate that the effect of microglia on OPC numbers may differ during development and adulthood, it is possible that the different findings are the result of the method of delivery (gavage), formulation, dosage, treatment duration, and pharmacokinetics of the BLZ945 inhibitor. The method of OPC quantification may also play a role as OPC numbers in adult corpus callosum tallied by PDGFR immunocytochemistry and genetic labeling were distinct. The lack of direct effect of BLZ945 on OPC viability *in vitro* (Hagemeyer et al., 2017) may be due to the high specificity of the inhibitor (IC_{50} CSF1R: < 1 nM; IC_{50} PDGFRβ: > 1 μM) (Pyonteck et al., 2013) and the high concentration of PDGR-A (10 ng/ml, EC50- < 1 ng/ml) in the culture medium.

In summary, by comparing the effect of PLX5622 and PLX3397, we confirm that CSF1R inhibitors can efficiently deplete microglia *ex vivo* and *in vivo* without affecting mature oligodendrocytes or myelin protein expression. In addition, we speculate that CSF1R inhibitors may directly impact OPC viability through off-target binding to PDGFRα, a member of the type III tyrosine kinase receptor family. Therefore, inhibitor concentration and duration of treatment must be carefully adjusted for the relevant experimental system. These data also question whether microglia are essential for OPC viability in *ex vivo* slice cultures and adult brain.

Declarations

All authors have been seen drafts of this manuscript and consent for publication. The datasets used and analyzed during the current study are available from the corresponding author on reasonable request.

Competing interests

The authors have no competing interests.

Funding

Author contributions

YL designed and coordinated the study, performed the experiments, analyzed the data, drafted the manuscript and revision. KS performed the experiments and analyzed the data. ED assisted in tissue sectioning and immunostaining experiments. GO reviewed the manuscript, WM and JB designed the study, reviewed the data and the manuscript.

Appendix A. Supplementary data

Supplementary data to this article can be found online at https://doi.org/10.1016/j.expneurol.2019.04.011.

References

Acharya, M.M., Green, K.N., Allen, B.D., Najafi, A.R., Syage, A., Minasyan, H., Le, M.T., Kawashita, T., Giedzinski, E., Parihar, V.K., West, B.L., Baulch, J.E., Limoli, C.L., 2016. Elimination of microglia improves cognitive function following cranial irradiation. Sci. Rep. 6, 31545.

Dagher, N.N., Najafi, A.R., Kayala, K.M., Elmore, M.R., White, T.E., Medeiros, R., West, B.L., Green, K.N., 2015. Colony-stimulating factor 1 receptor inhibition prevents microglial plaque association and improves cognition in 3xTg-AD mice. J. Neuroinflammation 12, 139.

DeNardo, D.G., Brennan, D.J., Rexhepaj, E., Ruffell, B., Shiao, S.L., Madden, S.F., Gallagher, W.M., Wadhwani, N., Keil, S.D., Junaid, S.A., Rugo, H.S., Hwang, E.S., Jirstrom, K., West, B.L., Coussens, L.M., 2011. Leukocyte complexity predicts breast cancer survival and functionally regulates response to chemotherapy. Cancer discovery 1, 54–67.

Elmore, M.R., Najafi, A.R., Koike, M.A., Dagher, N.N., Spangenberg, E.E., Rice, R.A., Kitazawa, M., Matusow, B., Nguyen, H., West, B.L., Green, K.N., 2014. Colony-stimulating factor 1 receptor signaling is necessary for microglia viability, unmasking a microglia progenitor cell in the adult brain. Neuron 82, 380–397.

Elmore, M.R., Lee, R.J., West, B.L., Green, K.N., 2015. Characterizing newly repopulated microglia in the adult mouse: impacts on animal behavior, cell morphology, and neuroinflammation. PLoS One 10, e0122912.

Grabert, K., Michoel, T., Karavolos, M.H., Clohisey, S., Baillie, J.K., Stevens, M.P., Freeman, T.C., Summers, K.M., McColl, B.W., 2016. Microglial brain region-dependent diversity and selective regional sensitivities to aging. Nat. Neurosci. 19, 504–516.

Hagemeyer, N., Hanft, K.M., Akriditou, M.A., Unger, N., Park, E.S., Stanley, E.R., Staszewski, O., Dimou, L., Prinz, M., 2017. Microglia contribute to normal myelinogenesis and to oligodendrocyte progenitor maintenance during adulthood. Acta Neuropathol. 134, 441–458.

Han, J., Harris, R.A., Zhang, X.M., 2017. An updated assessment of microglia depletion: current concepts and future directions. Molecular Brain 10, 25.

Kim, T.S., Cavnar, M.J., Cohen, N.A., Sorenson, E.C., Greer, J.B., Seifert, A.M., Crawley, M.H., Green, B.L., Popow, R., Pillarsetty, N., Veach, D.R., Ku, A.T., Rossi, F., Besmer, P., Antonescu, C.R., Zeng, S., Dematteo, R.P., 2014. Increased KIT inhibition enhances therapeutic efficacy in gastrointestinal stromal tumor. Clinical Cancer Research 20, 2350–2362.

Leite, C., Silva, N.T., Mendes, S., Ribeiro, A., de Faria, J.P., Lourenco, T., dos Santos, F., Andrade, P.Z., Cardoso, C.M., Vieira, M., Paiva, A., da Silva, C.L., Cabral, J.M., Relvas, J.B., Graos, M., 2014. Differentiation of human umbilical cord matrix mesenchymal stem cells into neural-like progenitor cells and maturation into an oligodendroglial-like lineage. PLoS One 9, e111059.

Li, M., Li, Z., Ren, H., Jin, W.N., Wood, K., Liu, Q., Sheth, K.N., Shi, F.D., 2017. Colony stimulating factor 1 receptor inhibition eliminates microglia and attenuates brain injury after intracerebral hemorrhage. J. Cereb. Blood Flow Metab. 37, 2383–2395.

Liu, Y., Harlow, D.E., Given, K.S., Owens, G.P., Macklin, W.B., Bennett, J.L., 2016. Variable sensitivity to complement-dependent cytotoxicity in murine models of neuromyelitis optica. J. Neuroinflammation 13, 301.

Mallon, B.S., Shick, H.E., Kidd, G.J., Macklin, W.B., 2002. Proteolipid promoter activity distinguishes two populations of NG2-positive cells throughout neonatal cortical development. J. Neurosci. 22, 876–885.

Matcovitch-Natan, O., Winter, D.R., Giladi, A., Vargas Aguilar, S., Spinrad, A., Sarrazin, S., Ben-Yehuda, H., David, E., Zelada Gonzalez, F., Perrin, P., Keren-Shaul, H., Gury, M., Lara-Astaiso, D., Thaiss, C.A., Cohen, M., Bahar Halpern, K., Baruch, K., Deczkowska, A., Lorenzo-Vivas, E., Itzkovitz, S., Elinav, E., Sieweke, M.H., Schwartz, M., Amit, I., 2016. Microglia development follows a stepwise program to regulate brain homeostasis. Science 353, aad8670.

Nishiyama, A., Komitova, M., Suzuki, R., Zhu, X., 2009. Polydendrocytes (NG2 cells): multifunctional cells with lineage plasticity. Nat. Rev. Neurosci. 10, 9–22.

Nissen, J.C., Thompson, K.K., West, B.L., Tsirka, S.E., 2018. Csf1R inhibition attenuates experimental autoimmune encephalomyelitis and promotes recovery. Exp. Neurol. 307, 24–36.

Peranzoni, E., Lemoine, J., Vimeux, L., Feuillet, V., Barrin, S., Kantari-Mimoun, C., Bercovici, N., Guerin, M., Biton, J., Ouakrim, H., Regnier, F., Lupo, A., Alifano, M., Damotte, D., Donnadieu, E., 2018. Macrophages impede CD8 T cells from reaching tumor cells and limit the efficacy of anti-PD-1 treatment. Proc. Natl. Acad. Sci. U. S. A. 115, E4041–E4050.

Pyonteck, S.M., Akkari, L., Schuhmacher, A.J., Bowman, R.L., Sevenich, L., Quail, D.F., Olson, O.C., Quick, M.L., Huse, J.T., Teijeiro, V., Setty, M., Leslie, C.S., Oei, Y., Pedraza, A., Zhang, J., Brennan, C.W., Sutton, J.C., Holland, E.C., Daniel, D., Joyce, J.A., 2013. CSF-1R inhibition alters macrophage polarization and blocks glioma progression. Nat. Med. 19, 1264–1272.

Rice, R.A., Pham, J., Lee, R.J., Najafi, A.R., West, B.L., Green, K.N., 2017. Microglial repopulation resolves inflammation and promotes brain recovery after injury. Glia 65, 931–944.

Robinson, D.R., Wu, Y.M., Lin, S.F., 2000. The protein tyrosine kinase family of the human genome. Oncogene 19, 5548–5557.

Salter, M.W., Stevens, B., 2017. Microglia emerge as central players in brain disease. Nat. Med. 23, 1018–1027.

Sheridan, G.K., Dev, K.K., 2012. S1P1 receptor subtype inhibits demyelination and regulates chemokine release in cerebellar slice cultures. Glia 60, 382–392.

Spangenberg, E.E., Lee, R.J., Najafi, A.R., Rice, R.A., Elmore, M.R., Blurton-Jones, M., West, B.L., Green, K.N., 2016. Eliminating microglia in Alzheimer's mice prevents neuronal loss without modulating amyloid-beta pathology. Brain 139, 1265–1281.

Szalay, G., Martinecz, B., Lenart, N., Kornyei, Z., Orsolits, B., Judak, L., Csaszar, E., Fekete, R., West, B.L., Katona, G., Rozsa, B., Denes, A., 2016. Microglia protect against brain injury and their selective elimination dysregulates neuronal network activity after stroke. Nat. Commun. 7, 11499.

Tap, W.D., Wainberg, Z.A., Anthony, S.P., Ibrahim, P.N., Zhang, C., Healey, J.H., Chmielowski, B., Staddon, A.P., Cohn, A.L., Shapiro, G.I., Keedy, V.L., Singh, A.S., Puzanov, I., Kwak, E.L., Wagner, A.J., Von Hoff, D.D., Weiss, G.J., Ramanathan, R.K., Zhang, J., Habets, G., Zhang, Y., Burton, E.A., Visor, G., Sanftner, L., Severson, P., Nguyen, H., Kim, M.J., Marimuthu, A., Tsang, G., Shellooe, R., Gee, C., West, B.L., Hirth, P., Nolop, K., van de Rijn, M., Hsu, H.H., Peterfy, C., Lin, P.S., Tong-Starksen, S., Bollag, G., 2015. Structure-guided blockade of CSF1R kinase in tenosynovial giant-cell tumor. N. Engl. J. Med. 373, 428–437.

Yamamura, T., Konola, J.T., Wekerle, H., Lees, M.B., 1991. Monoclonal antibodies against myelin proteolipid protein: identification and characterization of two major determinants. J. Neurochem. 57, 1671–1680.